nature medicine

Inhibition of Notch uncouples Akt activation from hepatic lipid accumulation by decreasing mTorc1 stability

Utpal B Pajvani[1], Li Qiang[1], Thaned Kangsamaksin[2–4], Jan Kitajewski[2,3], Henry N Ginsberg[1] & Domenico Accili[1]

Increased hepatic lipid content is an early correlate of insulin resistance and can be caused by nutrient-induced activation of mammalian target of rapamycin (mTor). This activation of mTor increases basal Akt activity, leading to a self-perpetuating lipogenic cycle. We have previously shown that the developmental Notch pathway has metabolic functions in adult mouse liver. Acute or chronic inhibition of Notch dampens hepatic glucose production and increases Akt activity and may therefore be predicted to increase hepatic lipid content. Here we now show that constitutive liver-specific ablation of Notch signaling, or its acute inhibition with a decoy Notch1 receptor, prevents hepatosteatosis by blocking mTor complex 1 (mTorc1) activity. Conversely, Notch gain of function causes fatty liver through constitutive activation of mTorc1, an effect that is reversible by treatment with rapamycin. We demonstrate that Notch signaling increases mTorc1 complex stability, augmenting mTorc1 function and sterol regulatory element binding transcription factor 1c (Srebp1c)-mediated lipogenesis. These data identify Notch as a therapeutically actionable branch point of metabolic signaling at which Akt activation in the liver can be uncoupled from hepatosteatosis.

Obesity-induced metabolic diseases, including type 2 diabetes and nonalcoholic fatty liver disease, will be a defining healthcare issue of the 21st century[1]. Aside from surgical remediation, progress in the treatment of these diseases with lifestyle or pharmacologic therapies has been disappointing.

Under normal physiological conditions, activation of the nutrient-sensing mTorc1 pathway, a substrate of insulin-Akt signaling[2], stimulates hepatic *de novo* lipogenesis[3]. For example, treatment of hepatocytes with rapamycin, an allosteric inhibitor of mTorc1, prevents insulin activation of the lipogenic transcription factor *Srebp1c* (also known as *Srebf1*)[3,4], and liver-specific knockout of the mTorc1-defining component Raptor protects from diet-induced hepatosteatosis, probably as a result of reduced lipogenesis[5]. At the same time, insulin-Akt signaling also acts to repress the action of forkhead box O1 (Foxo1) to suppress hepatic gluconeogenesis[6], defining the fasting-refeeding transition[7]. In obesity-induced hepatic insulin resistance, however, these parallel pathways become dissociated[3]. Specifically, Foxo1 action is unrestrained in the 'insulin-resistant' state to stimulate gluconeogenesis and glycogenolysis, and the resultant higher plasma insulin levels accelerate flux through the preserved Akt-mTorc1 pathway to simultaneously promote hepatic glucose production and hepatosteatosis—the latter being a correlate of cirrhosis, hepatocellular cancer and a need for liver transplantation[8]. The bifurcation of the insulin signaling pathways after Akt—to Foxo1 for glucose production and to mTorc1 and Srebp1c for lipogenesis—raises the question of whether these pathways have additional inputs. Here we explore further the role of Notch signaling in metabolic homeostasis of the liver.

Notch signaling is crucial for cell-type specification and lineage restriction[9]. Cell surface–tethered ligands (Jagged and Delta-like) bind Notch receptors on neighboring cells, resulting in a series of cleavage events that culminate in γ-secretase–dependent liberation of the Notch intracellular domain (NICD)[10]. The NICD translocates to the nucleus, where it binds to and coactivates the transcriptional effector Rbp-Jk, promoting expression of the *Hes* (hairy enhancer of split) and *Hey* (*Hes*-related) family of genes[11]. Homozygous null alleles of components of this signaling pathway result in embryonic lethality, demonstrating their importance in normal development[12–14]. Notch signaling is therapeutically accessible, and inhibitors are currently in advanced clinical development for cancer[15].

The homeostatic functions of Notch in developed tissues have received less attention, with the exception of neoplastic processes[16]. We have previously shown that Notch signaling in the liver is regulated in response to metabolic stimuli and that Notch1 increases hepatic glucose production by coactivating Foxo1 at the *G6pc* (encoding glucose-6-phosphatase) promoter[17]. Conversely, liver-specific deletion of Rbp-Jk in mice (resulting in mice called *L-Rbpj* mice) or treatment with a γ-secretase inhibitor (GSI) improves glucose tolerance and reduces hepatocyte glucose production[17]. As prior studies have demonstrated that Notch1 can activate mTorc1 in leukemic cells, whereas GSIs decrease mTorc1 activity in breast cancer[18,19], we hypothesized that hepatic Notch can modulate the coordinate actions of insulin on gluconeogenesis (through Foxo1) and lipogenesis (through mTorc1). Indeed, we found that inhibition of hepatic Notch protects from obesity-induced fatty liver, probably through decreased *de novo* lipogenesis. Conversely, constitutive hepatic Notch signaling stabilizes and activates mTorc1, leading to increased lipogenesis and fatty liver. We show that Notch-mediated hepatosteatosis is rapamycin sensitive, whereas Notch-induced glucose intolerance is mTor

[1]Department of Medicine, Columbia University, New York, New York, USA. [2]Department of Pathology, Columbia University, New York, New York, USA. [3]Department of Obstetrics and Gynecology, Columbia University, New York, New York, USA. [4]Present address: Department of Biochemistry, Faculty of Science, Mahidol University, Bangkok, Thailand. Correspondence should be addressed to U.B.P (up2104@columbia.edu) or D.A. (da230@columbia.edu).

Received 24 January; accepted 4 April; published online 7 July 2013; doi:10.1038/nm.3259

independent. These results establish Notch as a unique pharmacological target in liver whose inhibition can prevent the twin abnormalities of hepatic insulin resistance—excessive glucose production and fatty liver—through its ability to uncouple Akt signaling from mTor activation.

RESULTS

Liver Notch activity is altered by nutrient state

Notch1 activation in liver, as reflected by cleavage at Val1744 and increased expression of Notch target genes, increases with fasting[17]. When we analyzed wild-type mice after overnight fasting, we found that refeeding quickly (0–2 h) repressed Notch1 cleavage and target gene expression, but this decline was followed by a second peak of Notch activation at later time points (4–12 h) (**Fig. 1a** and **Supplementary Fig. 1**). Notably, Notch activation during fasting coincided with increased gluconeogenic gene expression, whereas the second peak coincided with maximal expression of *Srebp1c* and its transcriptional targets (*Fasn* (fatty acid synthase) and *Acc1* (acetyl-CoA carboxylase)) (**Fig. 1b–d**), as well as activation of mTor (data not shown). Notch target gene induction was absent in livers from mice lacking hepatocyte Rbp-Jk (*L-Rbpj* mice) (**Fig. 1e**)[17], confirming that classical Notch activation is affected by the nutritional state.

We hypothesized that nutrient excess would similarly stimulate hepatic Notch signaling. We analyzed livers from mice fed a high-fat diet (HFD), which showed greater Notch activation than those of chow-fed littermates (**Fig. 1f,g**), as did hepatocytes and livers from leptin signaling–deficient mice as compared to those from normal mice (**Fig. 1h,i**).

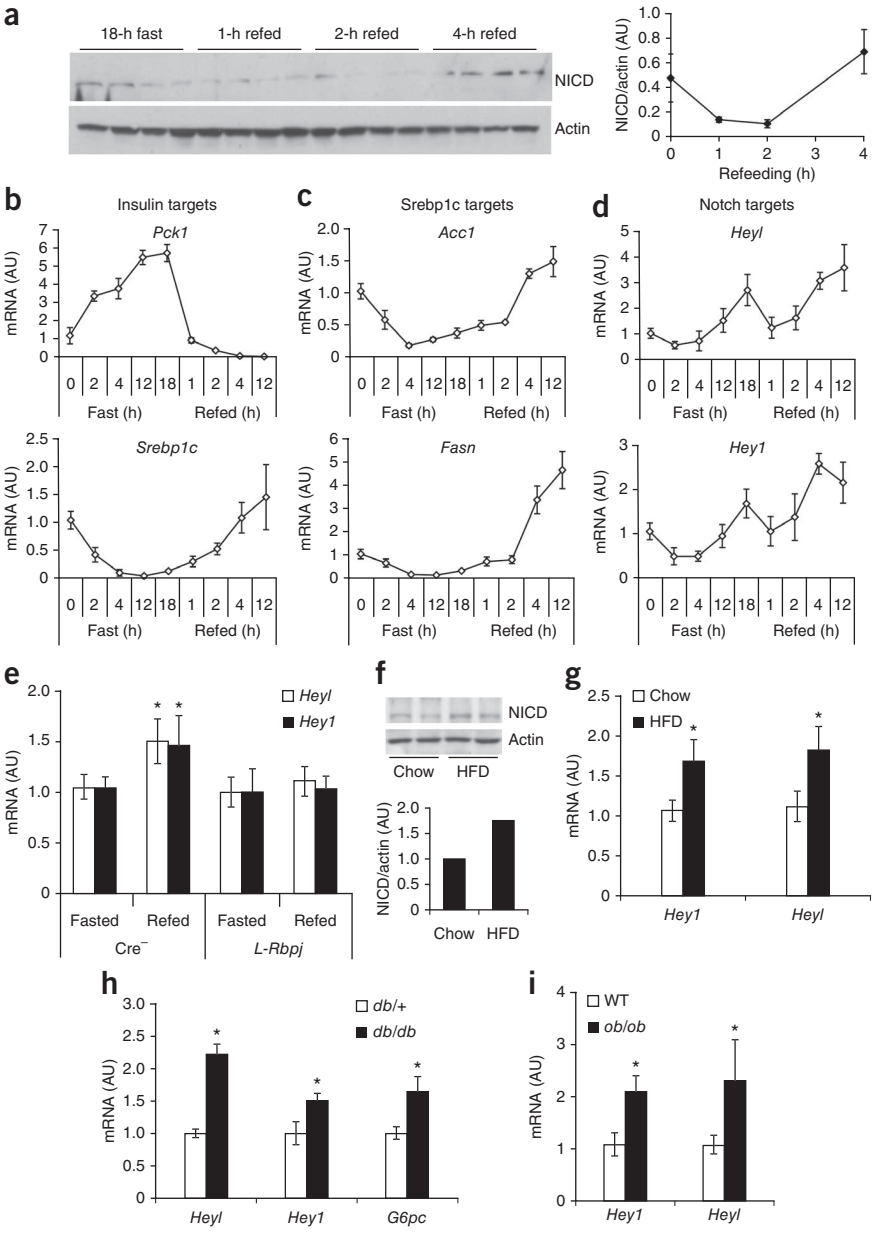

Figure 1 Regulation of hepatic Notch activity. (**a**) Western blot analysis and quantification of the cleaved Notch1 receptor (NICD) in livers from fasted and refed 9-week-old, chow-fed C57BL/6 mice ($n = 4$ per group). AU, arbitrary units. (**b–d**) Expression of insulin (**b**), Srebp1c (**c**) and Notch (**d**) targets in livers from fasted and refed 9-week-old, chow-fed C57BL/6 mice ($n = 5$ per group). (**e**) Regulation of Notch targets in 16-week-old *L-Rbpj* and control (Cre^-) mice fasted for 16 h or fasted for 16 h followed by a 4-h refeeding ($n = 6$ per group). The fasted values are set arbitrarily to 1 for both groups. $^*P < 0.05$ compared to fasted mice (two-way analysis of variance (ANOVA)). (**f,g**) Western blot analysis of cleaved Notch1 (**f**) and Notch target gene (**g**) expression in livers from fasted 16-week-old chow-fed or HFD-fed mice ($n = 12$ per group). $^*P < 0.05$ compared to chow-fed mice (two-way ANOVA). (**h,i**) Notch target expression in livers from *db/db* or control (*db*/+) mice ($n = 5$ per group; **h**) or in hepatocytes from *ob/ob* or control (wild-type (WT)) mice (**i**), all of which were analyzed after being in the *ad libitum* state (triplicate wells representative of two individual experiments). $^*P < 0.05$ compared to *db*/+ or WT mice (two-way ANOVA). All data are shown as the mean ± s.e.m.

These results suggest a cell-autonomous dysregulation of Notch signaling in obesity and fatty liver.

L-Rbpj mice show resistance to diet-induced fatty liver

As whole-body disruption of Rbp-Jk results in embryonic lethality[13], we generated mice harboring a liver-specific knockout (L-Rbpj) in which hepatocyte Rbp-Jk was deleted postnatally[17] and that had full recombination by 6–12 weeks of age[20]. We have previously shown that *L-Rbpj* mice are protected from obesity-induced insulin resistance[17]. Given the interaction between Rbp-Jk and Foxo1 (ref. 21), we hypothesized that *L-Rbpj* mice would have similarly increased hepatic triglyceride levels as mice lacking liver Foxo proteins[22,23]. Notably, despite unchanged body weight, *L- Rbpj* mice showed lower HFD-induced hepatic steatosis (**Fig. 2a,b**) that was due to a 30–50% reduction in hepatic triglyceride level (**Fig. 2c**). The livers of *L-Rbpj* mice were smaller, without changes in adiposity (**Fig. 2d**) or serum lipid concentrations (**Supplementary Fig. 2**), as compared to those

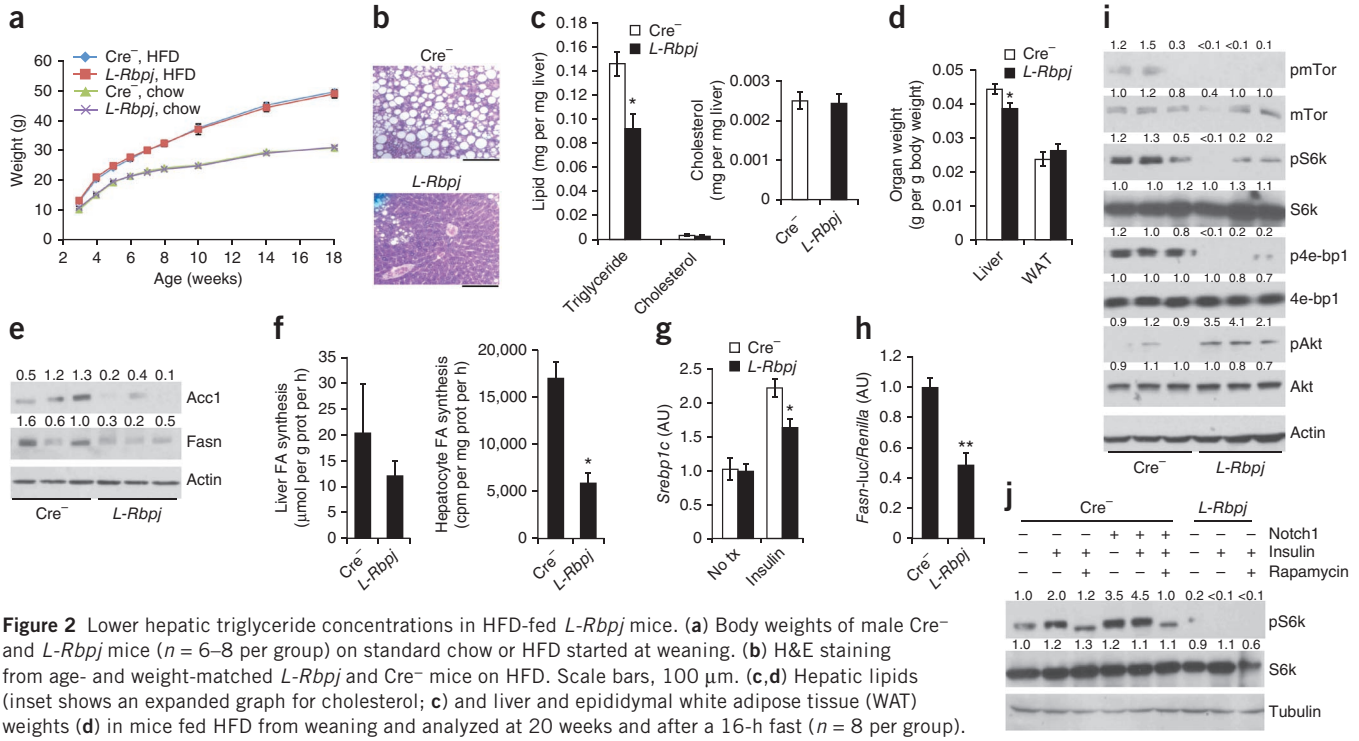

Figure 2 Lower hepatic triglyceride concentrations in HFD-fed *L-Rbpj* mice. (**a**) Body weights of male Cre⁻ and *L-Rbpj* mice ($n = 6$–8 per group) on standard chow or HFD started at weaning. (**b**) H&E staining from age- and weight-matched *L-Rbpj* and Cre⁻ mice on HFD. Scale bars, 100 μm. (**c**,**d**) Hepatic lipids (inset shows an expanded graph for cholesterol; **c**) and liver and epididymal white adipose tissue (WAT) weights (**d**) in mice fed HFD from weaning and analyzed at 20 weeks and after a 16-h fast ($n = 8$ per group). (**e**,**f**) Hepatic lipogenic protein expression (**e**) and *de novo* lipogenesis (**f**, left) in livers from 20-week-old, HFD-fed mice analyzed after a 16-h fast followed by a 6-h refeeding ($n = 7$ per group). FA, fatty acid; prot, protein. (**f**, right) *De novo* lipogenesis in hepatocytes from chow-fed *L-Rbpj* and Cre⁻ 16-week-old mice (triplicate wells representative of two individual experiments). cpm, counts per million. (**g**,**h**) Basal and insulin-stimulated *Srebp1c* expression (**g**) and *Fasn*-luciferase (*Fasn*-luc) activity (**h**) in primary hepatocytes from chow-fed 16-week-old Cre⁻ and *L-Rbpj* littermates that were transferred to serum-free medium for 16 h followed by the addition of 10 nM insulin for 6 h before lysis (triplicate wells representative of two individual experiments). tx, treatment. (**i**) Western blot analysis of Akt and mTor signaling in livers from HFD-fed mice analyzed after a 5-h fast. (**j**) Western blot analysis of hepatocytes isolated from 16-week-old *L-Rbpj* and Cre⁻ mice transduced with control or N1-IC adenovirus and treated with 10 nM insulin with or without 25 nM rapamycin for 4 h. Protein expression was normalized to either actin or tubulin. $^*P < 0.05$, $^{**}P < 0.01$ compared to Cre⁻ mice or hepatocytes (two-way ANOVA). All data are shown as the means ± s.e.m.

of Cre⁻ control mice. Moreover, Rbp-Jk knockout prevented steatosis in mice lacking hepatic Foxo1 (**Supplementary Fig. 3a**)[22], suggesting that Notch regulates hepatic lipid deposition independently of its known coactivation of Foxo1 targets[17].

To understand the lower hepatic triglyceride content in *L-Rbpj* mice, we systematically evaluated cell-autonomous and non–cell autonomous pathways that regulate hepatic triglyceride accumulation[8,24]. Very low density lipoprotein secretion was unaltered in *L-Rbpj* mice (**Supplementary Fig. 3b**), as were plasma triglyceride concentrations, after olive oil gavage (**Supplementary Fig. 3c**). Liver expression of the fatty acid oxidation enzymes encoded by *Acox* and *Cpt1a*, serum ketone concentrations and β-oxidation of exogenous fatty acids in primary hepatocytes were similarly unchanged (**Supplementary Fig. 3d–f**). Next we studied lipogenesis and found that the livers of *L-Rbpj* mice showed lower expression of Fasn and Acc1 compared to those of Cre⁻ control mice (**Fig. 2e**), leading to less fatty acid synthesis (**Fig. 2f**). In primary hepatocytes derived from *L-Rbpj* mice, we found impaired insulin-dependent *Srebp1c* expression and activity as assessed by lower expression of *Fasn* promoter–driven luciferase containing a consensus Srebp1c binding site[25] (**Fig. 2g**,**h**). Alternative lipogenic pathways, including peroxisome proliferator activated receptor γ (Ppar-γ) signaling[26], were unaltered in *L-Rbpj* mice (**Supplementary Fig. 3g**). We observed a similar protection from insulin resistance associated with lower hepatic triglyceride concentrations after short-term HFD feeding (**Supplementary Fig. 4**). These data indicate that blocking hepatic Notch reduces hepatic triglyceride concentrations, probably because of impaired Srebp1c-mediated lipogenesis.

We next studied two pathways that converge on Srebp1c: the insulin-Akt pathway and the nutrient-mTorc1 pathway[3]. Livers of *L-Rbpj* mice show higher insulin sensitivity with higher Akt phosphorylation at the Pdk1 site, Thr308 (ref. 17). Conversely, we noted repressed mTorc1 signaling, as indicated by lower phosphorylation of the mTor and mTorc1 targets, p70 S6 kinase (S6k) and 4e-bp1, after either 5 h or 16 h of fasting as compared to Cre⁻ control mice (**Fig. 2i** and data not shown)[27–29]. To determine whether this effect was cell autonomous, we isolated primary hepatocytes from Cre⁻ and *L-Rbpj* mice and found that although Akt phosphorylation was higher in the hepatocytes from the *L-Rbpj* mice (data not shown), basal and insulin-stimulated p70 S6k phosphorylation were repressed (**Fig. 2j**). These data suggest that Notch is required for maximal hepatocyte mTorc1 activity.

Notch1 decoy reduces insulin resistance and fatty liver

To exclude the possibility of a developmental phenotype in *L-Rbpj* mice, we transduced adult mice with a Notch1 receptor that encodes only the extracellular domain[30,31] and acts in a dominant-negative manner by sequestering endogenous ligands. This adenovirus-driven Notch1 decoy is preferentially expressed in the liver, blocks hepatic Notch target gene expression and is poorly secreted into the circulation (data not shown). Consistent with the results from the *L-Rbpj* mice, expression of the Notch1 decoy in HFD-fed mice lowered glucose

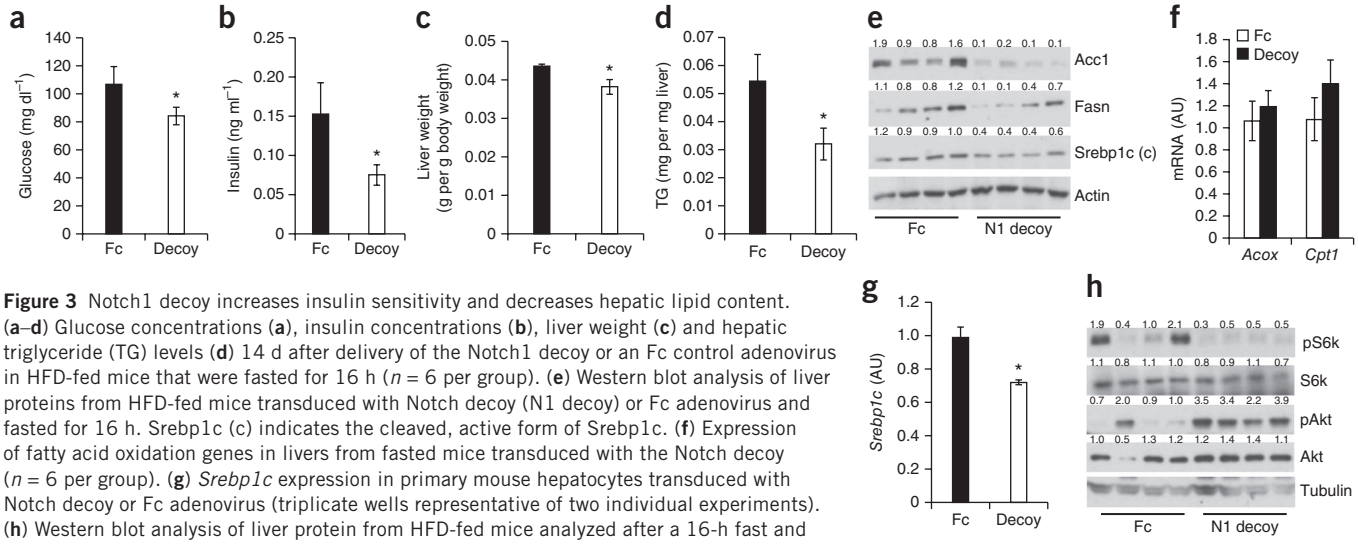

Figure 3 Notch1 decoy increases insulin sensitivity and decreases hepatic lipid content. (**a**–**d**) Glucose concentrations (**a**), insulin concentrations (**b**), liver weight (**c**) and hepatic triglyceride (TG) levels (**d**) 14 d after delivery of the Notch1 decoy or an Fc control adenovirus in HFD-fed mice that were fasted for 16 h ($n = 6$ per group). (**e**) Western blot analysis of liver proteins from HFD-fed mice transduced with Notch decoy (N1 decoy) or Fc adenovirus and fasted for 16 h. Srebp1c (c) indicates the cleaved, active form of Srebp1c. (**f**) Expression of fatty acid oxidation genes in livers from fasted mice transduced with the Notch decoy ($n = 6$ per group). (**g**) *Srebp1c* expression in primary mouse hepatocytes transduced with Notch decoy or Fc adenovirus (triplicate wells representative of two individual experiments). (**h**) Western blot analysis of liver protein from HFD-fed mice analyzed after a 16-h fast and transduced with Notch decoy or Fc adenovirus. Protein expression was normalized to either actin or tubulin. The mice analyzed were 12-week-old male C57BL/6 mice unless otherwise indicated. $^*P < 0.05$ compared to Fc adenovirus (two-way ANOVA). All data are shown as the means ± s.e.m.

and insulin concentrations (**Fig. 3a**,**b**), liver weight and triglyceride content as compared to Cre$^-$ control mice (**Fig. 3c**,**d**) without affecting body or adipose weight (**Supplementary Fig. 5a**,**b**).

We next tested whether acute inhibition of Notch signaling can protect from diet-induced fatty liver and reduce mTorc1 function commensurate with that in *L-Rbpj* mice. Notch1 decoy inhibited Srebp1c cleavage and the expression of Fasn and Acc1 (**Fig. 3e**) but did not affect fatty acid oxidation (**Fig. 3f**) or serum lipid concentrations (**Supplementary Fig. 5c**,**d**). Notch1 decoy–transduced primary hepatocytes from wild-type mice similarly showed lower *Srebp1c* expression, as compared to hepatocytes transduced with control virus (**Fig. 3g**), but no change in the expression of *Pparg* or its targets (**Supplementary Fig. 5e**). Livers from Notch1 decoy–transduced mice demonstrated higher phosphorylation of Akt (pAkt) at Thr308 but lower pS6k at Ser389 (**Fig. 3h**). Thus, similar to the results in *L-Rbpj* mice, acute reduction in hepatic Notch signaling increases insulin sensitivity while simultaneously lowering mTorc1-mediated Srebp1c activity and hepatic triglyceride concentrations.

Hepatic Notch1 induces mTorc1 signaling and fatty liver

Our loss-of-function studies suggest that Notch signaling is permissive for mTorc1 activation and diet-induced steatosis. We thus tested whether Notch gain of function would be sufficient to induce fatty liver *in vivo*. Chow-fed mice transduced with an adenovirus encoding constitutively active Notch1 (N1-IC) showed higher liver weight and triglyceride levels than mice transduced with control (GFP) adenovirus (**Fig. 4a**–**c**) without concomitant changes in body weight or composition (data not shown). Livers from N1-IC adenovirus–transduced mice had higher Srebp1c cleavage, resulting in increased expression of *Srebp1c* and *Fasn* (**Fig. 4d**,**e**). Consequently, primary hepatocytes from mice transduced with the N1-IC adenovirus showed greater lipogenesis (**Supplementary Fig. 6a**). Notably, N1-IC expression did not alter lipogenic gene expression or hepatic triglyceride levels in *L-Rbpj* mice and hepatocytes or affect fatty-acid synthesis in hepatocytes derived from *L-Rbpj* mice (**Fig. 4f**,**g** and **Supplementary Fig. 6b**), suggesting that Notch-induced lipogenesis requires Rbp-Jk, which is similar to its activation of hepatic glucose production[17].

Notch-induced lipogenic gene expression paralleled higher hepatic mTorc1 activity in fasted and, more markedly, refed mice (**Fig. 4h**), which is consistent with enhanced physiologic regulation of mTorc1. In hepatoma cells and mouse primary hepatocytes, activation of mTorc1 signaling by insulin and amino acids was potentiated by N1-IC (**Fig. 4i**), resulting in Srebp1c cleavage and activation (**Fig. 4j** and **Supplementary Fig. 6c**). These data suggest that Notch modulates, but does not over-ride, endogenous mTor regulation in a cell-autonomous manner.

Inhibition of mTor prevents Notch-induced fatty liver

To test the hypothesis that Notch induction of lipogenic gene expression and fatty liver requires mTorc1 signaling, we cotransfected hepatoma cells with *Fasn*-luciferase and shRNA to Raptor[32], the defining component of the mTorc1 complex, and then transduced the cells with the N1-IC adenovirus. Notch-induction of *Fasn*-luciferase activity was potentiated by insulin but was reversed by Raptor knockdown or treatment with rapamycin (**Fig. 5a** and **Supplementary Fig. 7**). Similarly, Notch induction of endogenous *Fasn* in primary hepatocytes was augmented by insulin and suppressed by rapamycin (**Fig. 5b**), suggesting that N1-IC–induced *Fasn* expression is mTorc1 dependent.

On the basis of these data, we hypothesized that the higher lipogenic gene expression and fatty liver in mice transduced with N1-IC adenovirus would be ameliorated by rapamycin treatment. Indeed, Notch-mediated hepatic steatosis was completely reversed by rapamycin treatment (**Fig. 5c**). The effect of rapamycin was specific to Notch induction of lipogenic genes, as *Heyl* and *Hey1* were unaffected (**Fig. 5d**). Similarly, although rapamycin induced mild glucose intolerance (data not shown)[33], N1-IC adenovirus–transduced mice showed further exacerbation of glucose intolerance (**Fig. 5e**,**f**). These data show that Notch-induced hepatic steatosis, but not hyperglycemia, is prevented by mTor inhibition.

Notch increases mTorc1 complex stability

To study the mechanism of altered Notch-induced mTorc1 activation, we examined mTor component expression in livers of HFD-fed *L-Rbpj* mice. We found unchanged levels of the shared mTorc1 and mTorc2 components, mTor and Gβl, and the mTorc2-specific component Rictor but a reduction in the levels of Raptor protein (**Fig. 6a**) independent of changes in *Raptor* mRNA levels (data not shown),

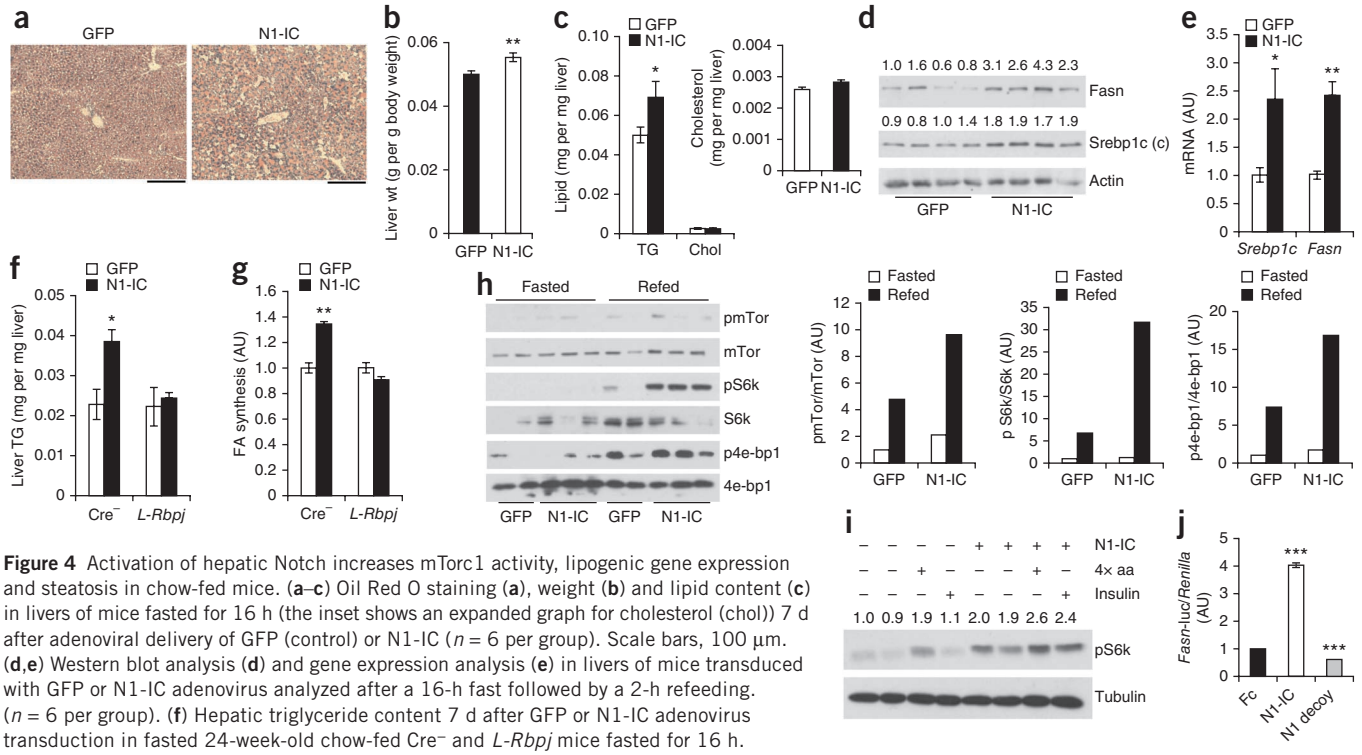

Figure 4 Activation of hepatic Notch increases mTorc1 activity, lipogenic gene expression and steatosis in chow-fed mice. (**a**–**c**) Oil Red O staining (**a**), weight (**b**) and lipid content (**c**) in livers of mice fasted for 16 h (the inset shows an expanded graph for cholesterol (chol)) 7 d after adenoviral delivery of GFP (control) or N1-IC ($n = 6$ per group). Scale bars, 100 μm. (**d**,**e**) Western blot analysis (**d**) and gene expression analysis (**e**) in livers of mice transduced with GFP or N1-IC adenovirus analyzed after a 16-h fast followed by a 2-h refeeding. ($n = 6$ per group). (**f**) Hepatic triglyceride content 7 d after GFP or N1-IC adenovirus transduction in fasted 24-week-old chow-fed Cre⁻ and *L-Rbpj* mice fasted for 16 h. (**g**) *De novo* lipogenesis in hepatocytes isolated from *L-Rbpj* and Cre⁻ mice after transduction with GFP (arbitrarily set to a value of 1) or N1-IC adenovirus and incubation with 10 nM insulin (triplicate wells representative of two individual experiments). (**h**) Western blot analysis and quantification of the bands from livers of mice transduced with GFP or N1-IC adenovirus and either fasted for 16 h or refed for 2 h. (**i**) Western blot analysis of FAO hepatoma cells transduced with Fc (–) or N1-IC adenovirus, incubated in serum-free and amino acid–free medium for 4 h and treated with 10 nM insulin or a 4× amino acid (aa) mixture for 4 h. (**j**) *Fasn*-luciferase assays in FAO hepatoma cells transduced with N1-IC, Notch1 decoy or Fc (control) adenovirus and treated with 10 nM insulin. $^*P < 0.05$, $^{**}P < 0.01$, $^{***}P < 0.001$ compared to Fc or GFP adenovirus (two-way ANOVA). Protein expression was normalized to either actin or tubulin. The mice analyzed were 8-week-old C57BL/6 males unless otherwise indicated. All data are shown as the means ± s.e.m.

suggesting that the effects of Rbp-Jk deficiency on Raptor are post-transcriptional. Conversely, mice transduced with N1-IC adenovirus demonstrated higher liver Raptor protein expression as compared to control mice transduced with GFP adenovirus (**Fig. 6b**). We found a similar increase in the amount of endogenous Raptor protein in hepatoma cells (**Fig. 6c**) and primary hepatocytes (data not shown) from mice transduced with the N1-IC adenovirus without changes in *Raptor* mRNA levels (**Supplementary Fig. 8a**). Transient transfection of Raptor cDNA in primary hepatocytes showed a similar effect, demonstrating that the action of Notch is independent of locus

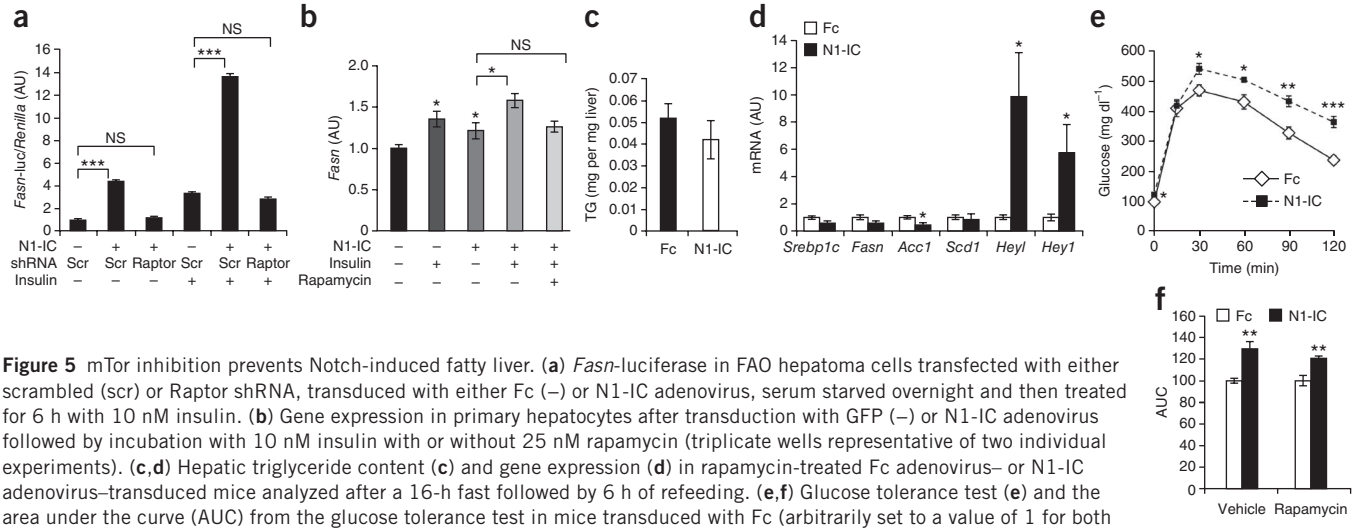

Figure 5 mTor inhibition prevents Notch-induced fatty liver. (**a**) *Fasn*-luciferase in FAO hepatoma cells transfected with either scrambled (scr) or Raptor shRNA, transduced with either Fc (–) or N1-IC adenovirus, serum starved overnight and then treated for 6 h with 10 nM insulin. (**b**) Gene expression in primary hepatocytes after transduction with GFP (–) or N1-IC adenovirus followed by incubation with 10 nM insulin with or without 25 nM rapamycin (triplicate wells representative of two individual experiments). (**c**,**d**) Hepatic triglyceride content (**c**) and gene expression (**d**) in rapamycin-treated Fc adenovirus– or N1-IC adenovirus–transduced mice analyzed after a 16-h fast followed by 6 h of refeeding. (**e**,**f**) Glucose tolerance test (**e**) and the area under the curve (AUC) from the glucose tolerance test in mice transduced with Fc (arbitrarily set to a value of 1 for both treatments) or N1-IC adenovirus and injected daily with rapamycin or vehicle. The mice analyzed were 10-week-old, short-term (3 weeks) HFD-fed C57BL/6 males. $^*P < 0.05$, $^{**}P < 0.01$, $^{***}P < 0.001$ compared to Fc adenovirus–transduced cells or mice (two-way ANOVA). NS, not significant. All data are shown as the means ± s.e.m.

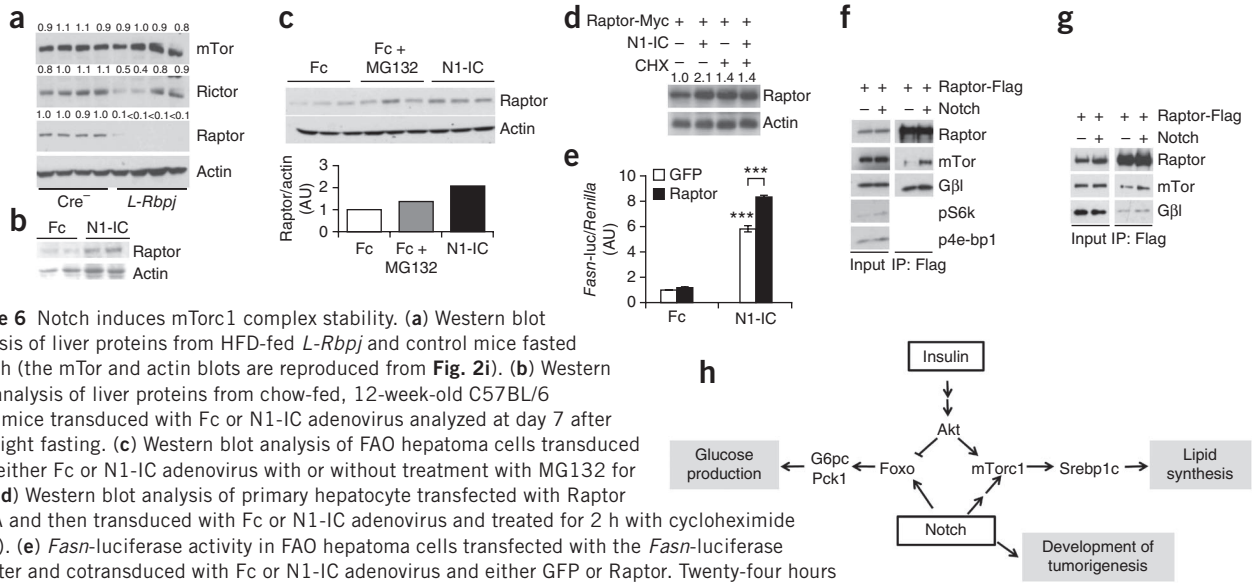

Figure 6 Notch induces mTorc1 complex stability. (**a**) Western blot analysis of liver proteins from HFD-fed *L-Rbpj* and control mice fasted for 5 h (the mTor and actin blots are reproduced from **Fig. 2i**). (**b**) Western blot analysis of liver proteins from chow-fed, 12-week-old C57BL/6 male mice transduced with Fc or N1-IC adenovirus analyzed at day 7 after overnight fasting. (**c**) Western blot analysis of FAO hepatoma cells transduced with either Fc or N1-IC adenovirus with or without treatment with MG132 for 4 h. (**d**) Western blot analysis of primary hepatocyte transfected with Raptor cDNA and then transduced with Fc or N1-IC adenovirus and treated for 2 h with cycloheximide (CHX). (**e**) *Fasn*-luciferase activity in FAO hepatoma cells transfected with the *Fasn*-luciferase reporter and cotransduced with Fc or N1-IC adenovirus and either GFP or Raptor. Twenty-four hours after transduction, hepatoma cells were transferred to serum-free medium for 16 h and then treated with 10 nM insulin for 6 h before lysis. $***P < 0.001$ compared to Fc adenovirus (two-way ANOVA). The data are shown as the means ± s.e.m. (**f**,**g**) Western blot analysis of HEK293 cells (**f**) or primary hepatocytes (**g**) transfected with Flag-tagged Raptor (Raptor-Flag) followed by transduction with GFP or N1-IC adenovirus and immunoprecipitation with Flag-specific antibody. Protein expression was normalized to either actin or tubulin. (**h**) Schematic diagram outlining the effects of Notch on hepatic glucose and lipid metabolism.

effects (**Supplementary Fig. 8b**). Notably, the effect of N1-IC was not recapitulated by proteosomal inhibition with MG132 (**Fig. 6c**) but was reversed by treatment of hepatocytes with the protein synthesis inhibitor cycloheximide (**Fig. 6d**).

Raptor overexpression was insufficient to induce *Fasn*-luciferase, whereas coexpression of N1-IC and Raptor produced a synergistic effect (**Fig. 6e**), which is consistent with previous work that Raptor overexpression does not increase mTorc1 function *per se*[34]. Likewise, overexpression of Raptor was insufficient to activate mTorc1 in either primary hepatocytes or HEK293 cells (data not shown). We conclude that Notch induction of Raptor expression parallels but does not cause increased mTorc1 activation and hypothesize that increased Raptor expression is secondary to higher mTorc1 complex stability. Indeed, we found that Notch overexpression increased the association among mTorc1 components in HEK293 cells (**Fig. 6f**) regardless of whether Raptor (**Supplementary Fig. 8c**) or mTor (**Supplementary Fig. 8d**) was immunoprecipitated. We observed similar mTorc1 stabilization in FAO hepatoma cells (**Supplementary Fig. 8e**) and mouse primary hepatocytes (**Fig. 6g**). In addition, Notch-stabilized mTorc1 complexes were resistant to increasing concentrations of CHAPS detergent, which is known to disrupt the mTor-Raptor interaction (**Supplementary Fig. 8f**)[34–36]. These data indicate that Notch stabilizes and activates mTorc1, resulting in increased *de novo* lipogenesis and fatty liver.

DISCUSSION

The role of developmental pathways in the metabolic homeostasis of adult tissues is only beginning to be appreciated[17,37]. We have shown that genetic or pharmacologic inhibition of Notch protects from diet-induced glucose intolerance in a Foxo1-dependent manner without effects on body weight or adiposity[17]. We demonstrate here a similar protection from fatty liver with inhibition of hepatic Notch signaling. We did not expect this result, as inhibition of hepatic Foxo1 is associated with increased hepatic lipid deposition[22,23,38], an effect of shifting hepatic carbon flux from glucose to lipid production, as has been seen in other recently described mouse models[39,40]. In this regard, it seems that chronic (as in *L-Rbpj* mice) or acute (using Notch decoy) Notch inhibition achieves the long-sought goal of decreasing hepatic glucose production without compensatory increases in hepatic lipid content. Notably, GSIs induce fatty liver, but they do so in a Notch-independent fashion (U.B.P., unpublished data), which is consistent with the idea that substrates of γ-secretase include Notch-unrelated pathways and restricts the repertoire of therapeutically viable Notch inhibitors that can be pursued for treatment of metabolic disease. Nonetheless, the many potential benefits of Notch inhibition, which include the amelioration of atherosclerosis[41], provide a strong rationale to pursue Notch inhibition as a treatment of the metabolic syndrome[42].

The identification of Notch as a regulator of carbon flux toward hepatic glucose or lipid production (**Fig. 6h**) is a conceptual advance, as is the finding that a molecular pathway thought to be specialized toward differentiation is regulated by physiologic (fasting and refeeding), as well as pathologic (insulin resistance), metabolic cues in hepatocytes. We hypothesize that in the overfed and insulin-resistant state, Notch signaling is inappropriately activated and reprises its developmental interactions with Foxo1 and mTorc1. The mechanisms underlying nutritional activation of hepatic Notch require further clarification. For example, it should be determined whether Notch activation in the hepatocyte requires input from neighboring hepatocytes or other resident liver cells (for example, endothelial, stellate or Kupffer cells, among others). Similarly, which of the five Notch ligands drives signaling in response to nutrients is unknown, and the possibility that different ligands signal in different metabolic states to direct carbon flux or drive differentiation is teleologically attractive.

Besides the further validation of hepatic Notch as a therapeutic target, our data demonstrate a physiologic, and potentially pharmacologic, means of regulating mTorc1 activity and lipogenesis. Previous studies have indicated that tight control of hepatic mTorc1 signaling is crucial for hepatic lipid metabolism[43,44]. The tandem, but not necessarily related, findings of mTorc1 stabilization and activation by Notch deserve further study. Since the identification of Raptor as the

mTorc1-regulatory subunit, it has been known that the mTor-Raptor association is sensitive to detergent concentrations[38]; subsequent reports have confirmed this finding and identified potential post-translational modifications of Raptor[35,36,45], but none of these modifications has been shown to mediate the mTor-Raptor interaction. How Notch induces mTorc1 stability is unknown, but the demonstration that Raptor protein, but not mRNA, expression is decreased in *L-Rbpj* mice and that cycloheximide prevents Notch-induced stabilization indicates that a transcriptional target(s) of Notch regulates complex stability.

In summary, Notch antagonism uncouples Akt from mTor activation, suggesting that Notch antagonists from oncology and neuroscience[46,47] may be repurposed to treat fatty liver and diabetes. Furthermore, as Notch-mediated mTorc1 activation does not seem to be cell-type specific, modulators of mTorc1 processing and degradation may be a therapeutic avenue to block mTorc1 activity without the metabolic liabilities of current mTor inhibitors[33,48].

METHODS

Methods and any associated references are available in the online version of the paper.

Note: Supplementary information is available in the online version of the paper.

ACKNOWLEDGMENTS

This work was supported by US National Institutes of Health grants DK093604 (U.B.P.), DK57539 (D.A.), HL062454 (J.K.) and DK63608 (Columbia Diabetes Research Center). We thank D. Conlon, C. Eng, I. Goldberg, R. Haeusler and I. Tabas, as well as members of the Accili, Kitajewski and Ginsberg laboratories, for insightful discussion of the data. We acknowledge excellent technical support from A. Flete, T. Kolar and J. Lee, as well as plasmids from D. Sabatini (Whitehead Institute) and B. Spiegelman (Dana-Farber Cancer Institute).

AUTHOR CONTRIBUTIONS

U.B.P. designed and performed experiments, analyzed data and wrote the manuscript. L.Q. and T.K. designed and performed experiments and analyzed data. J.K., H.N.G. and D.A. designed the studies, analyzed the data and wrote the manuscript.

COMPETING FINANCIAL INTERESTS

The authors declare no competing financial interests.

1. Wang, Y.C., McPherson, K., Marsh, T., Gortmaker, S.L. & Brown, M. Health and economic burden of the projected obesity trends in the USA and the UK. *Lancet* **378**, 815–825 (2011).
2. Hay, N. & Sonenberg, N. Upstream and downstream of mTOR. *Genes Dev.* **18**, 1926–1945 (2004).
3. Li, S., Brown, M.S. & Goldstein, J.L. Bifurcation of insulin signaling pathway in rat liver: mTORC1 required for stimulation of lipogenesis, but not inhibition of gluconeogenesis. *Proc. Natl. Acad. Sci. USA* **107**, 3441–3446 (2010).
4. Sabatini, D.M. mTOR and cancer: insights into a complex relationship. *Nat. Rev. Cancer* **6**, 729–734 (2006).
5. Peterson, T.R. *et al.* mTOR complex 1 regulates lipin 1 localization to control the SREBP pathway. *Cell* **146**, 408–420 (2011).
6. Matsumoto, M., Pocai, A., Rossetti, L., Depinho, R.A. & Accili, D. Impaired regulation of hepatic glucose production in mice lacking the forkhead transcription factor Foxo1 in liver. *Cell Metab.* **6**, 208–216 (2007).
7. Matsumoto, M., Han, S., Kitamura, T. & Accili, D. Dual role of transcription factor Foxo1 in controlling hepatic insulin sensitivity and lipid metabolism. *J. Clin. Invest.* **116**, 2464–2472 (2006).
8. Savage, D.B. & Semple, R.K. Recent insights into fatty liver, metabolic dyslipidaemia and their links to insulin resistance. *Curr. Opin. Lipidol.* **21**, 329–336 (2010).
9. Bolós, V., Grego-Bessa, J. & de la Pompa, J.L. Notch signaling in development and cancer. *Endocr. Rev.* **28**, 339–363 (2007).
10. Fortini, M.E. Notch signaling: the core pathway and its posttranslational regulation. *Dev. Cell* **16**, 633–647 (2009).
11. Dufraine, J., Funahashi, Y. & Kitajewski, J. Notch signaling regulates tumor angiogenesis by diverse mechanisms. *Oncogene* **27**, 5132–5137 (2008).
12. Swiatek, P.J., Lindsell, C.E., del Amo, F.F., Weinmaster, G. & Gridley, T. Notch1 is essential for postimplantation development in mice. *Genes Dev.* **8**, 707–719 (1994).
13. Oka, C. *et al.* Disruption of the mouse RBP-Jκ gene results in early embryonic death. *Development* **121**, 3291–3301 (1995).
14. Shen, J. *et al.* Skeletal and CNS defects in Presenilin-1–deficient mice. *Cell* **89**, 629–639 (1997).
15. Rizzo, P. *et al.* Rational targeting of Notch signaling in cancer. *Oncogene* **27**, 5124–5131 (2008).
16. Weinmaster, G. & Kopan, R. A garden of Notch-ly delights. *Development* **133**, 3277–3282 (2006).
17. Pajvani, U.B. *et al.* Inhibition of Notch signaling ameliorates insulin resistance in a Foxo1-dependent manner. *Nat. Med.* **17**, 961–967 (2011).
18. Chan, S.M., Weng, A.P., Tibshirani, R., Aster, J.C. & Utz, P.J. Notch signals positively regulate activity of the mTOR pathway in T-cell acute lymphoblastic leukemia. *Blood* **110**, 278–286 (2007).
19. Efferson, C.L. *et al.* Downregulation of Notch pathway by a γ-secretase inhibitor attenuates AKT/mammalian target of rapamycin signaling and glucose uptake in an ERBB2 transgenic breast cancer model. *Cancer Res.* **70**, 2476–2484 (2010).
20. Postic, C. & Magnuson, M.A. DNA excision in liver by an albumin-Cre transgene occurs progressively with age. *Genesis* **26**, 149–150 (2000).
21. Kitamura, T. *et al.* A Foxo/Notch pathway controls myogenic differentiation and fiber type specification. *J. Clin. Invest.* **117**, 2477–2485 (2007).
22. Haeusler, R.A., Pratt-Hyatt, M., Welch, C.L., Klaassen, C.D. & Accili, D. Impaired generation of 12-hydroxylated bile acids links hepatic insulin signaling with dyslipidemia. *Cell Metab.* **15**, 65–74 (2012).
23. Tao, R. *et al.* Hepatic FoxOs regulate lipid metabolism via modulation of expression of the nicotinamide phosphoribosyltransferase gene. *J. Biol. Chem.* **286**, 14681–14690 (2011).
24. Postic, C. & Girard, J. Contribution of *de novo* fatty acid synthesis to hepatic steatosis and insulin resistance: lessons from genetically engineered mice. *J. Clin. Invest.* **118**, 829–838 (2008).
25. Kim, J.B., Wright, H.M., Wright, M. & Spiegelman, B.M. ADD1/SREBP1 activates PPARγ through the production of endogenous ligand. *Proc. Natl. Acad. Sci. USA* **95**, 4333–4337 (1998).
26. Zhang, Y.L. *et al.* Aberrant hepatic expression of PPARγ2 stimulates hepatic lipogenesis in a mouse model of obesity, insulin resistance, dyslipidemia, and hepatic steatosis. *J. Biol. Chem.* **281**, 37603–37615 (2006).
27. Gingras, A.C. *et al.* Regulation of 4E-BP1 phosphorylation: a novel two-step mechanism. *Genes Dev.* **13**, 1422–1437 (1999).
28. Chiang, G.G. & Abraham, R.T. Phosphorylation of mammalian target of rapamycin (mTOR) at Ser-2448 is mediated by p70S6 kinase. *J. Biol. Chem.* **280**, 25485–25490 (2005).
29. Weng, Q.P. *et al.* Regulation of the p70 S6 kinase by phosphorylation *in vivo*. Analysis using site-specific anti-phosphopeptide antibodies. *J. Biol. Chem.* **273**, 16621–16629 (1998).
30. Funahashi, Y. *et al.* A notch1 ectodomain construct inhibits endothelial notch signaling, tumor growth, and angiogenesis. *Cancer Res.* **68**, 4727–4735 (2008).
31. Funahashi, Y. *et al.* Notch modulates VEGF action in endothelial cells by inducing matrix metalloprotease activity. *Vasc. Cell* **3**, 2 (2011).
32. Peterson, T.R. *et al.* DEPTOR is an mTOR inhibitor frequently overexpressed in multiple myeloma cells and required for their survival. *Cell* **137**, 873–886 (2009).
33. Blättler, S.M. *et al.* Yin Yang 1 deficiency in skeletal muscle protects against rapamycin-induced diabetic-like symptoms through activation of insulin/IGF signaling. *Cell Metab.* **15**, 505–517 (2012).
34. Kim, D.H. *et al.* mTOR interacts with raptor to form a nutrient-sensitive complex that signals to the cell growth machinery. *Cell* **110**, 163–175 (2002).
35. Foster, K.G. *et al.* Regulation of mTOR complex 1 (mTORC1) by raptor Ser863 and multisite phosphorylation. *J. Biol. Chem.* **285**, 80–94 (2010).
36. Kaizuka, T. *et al.* Tti1 and Tel2 are critical factors in mammalian target of rapamycin complex assembly. *J. Biol. Chem.* **285**, 20109–20116 (2010).
37. Liu, H. *et al.* Wnt signaling regulates hepatic metabolism. *Sci. Signal.* **4**, ra6 (2011).
38. Haeusler, R.A., Kaestner, K.H. & Accili, D. FoxOs function synergistically to promote glucose production. *J. Biol. Chem.* **285**, 35245–35248 (2010).
39. Sun, Z. *et al.* Hepatic Hdac3 promotes gluconeogenesis by repressing lipid synthesis and sequestration. *Nat. Med.* **18**, 934–942 (2012).
40. Hagiwara, A. *et al.* Hepatic mTorc2 activates glycolysis and lipogenesis through Akt, glucokinase, and SREBP1c. *Cell Metab.* **15**, 725–738 (2012).
41. Fukuda, D. *et al.* Notch ligand Delta-like 4 blockade attenuates atherosclerosis and metabolic disorders. *Proc. Natl. Acad. Sci. USA* **109**, E1868–E1877 (2012).
42. Kim-Muller, J.Y. & Accili, D. Cell biology. Selective insulin sensitizers. *Science* **331**, 1529–1531 (2011).
43. Howell, J.J. & Manning, B.D. mTOR couples cellular nutrient sensing to organismal metabolic homeostasis. *Trends Endocrinol. Metab.* **22**, 94–102 (2011).
44. Yecies, J.L. *et al.* Akt stimulates hepatic SREBP1c and lipogenesis through parallel mTORC1-dependent and independent pathways. *Cell Metab.* **14**, 21–32 (2011).
45. Gwinn, D.M. *et al.* AMPK phosphorylation of raptor mediates a metabolic checkpoint. *Mol. Cell* **30**, 214–226 (2008).
46. Noguera-Troise, I. *et al.* Blockade of Dll4 inhibits tumour growth by promoting non-productive angiogenesis. *Nature* **444**, 1032–1037 (2006).
47. Wu, Y. *et al.* Therapeutic antibody targeting of individual Notch receptors. *Nature* **464**, 1052–1057 (2010).
48. Houde, V.P. *et al.* Chronic rapamycin treatment causes glucose intolerance and hyperlipidemia by upregulating hepatic gluconeogenesis and impairing lipid deposition in adipose tissue. *Diabetes* **59**, 1338–1348 (2010).

ONLINE METHODS

Antibodies. We purchased antibodies to pAkt1 (http://www.cellsignal.com/products/2965.html), p70 pS6k (http://www.cellsignal.com/products/9205.html), total p70 S6k (http://www.cellsignal.com/products/9202.html), pmTor (http://www.cellsignal.com/products/5536.html), total mTor (http://www.cellsignal.com/products/2983.html), p4e-bp1 (http://www.cellsignal.com/products/2855.html), total 4e-bp1 (http://www.cellsignal.com/products/9644.html), Raptor (http://www.cellsignal.com/products/2280.html), Rictor (http://www.cellsignal.com/products/2114.html), Gβl (http://www.cellsignal.com/products/3274.html), fatty acid synthase (http://www.cellsignal.com/products/3189.html), acetyl-CoA carboxylase (http://www.cellsignal.com/products/3676.html), tubulin (http://www.cellsignal.com/products/2148.html) and actin (http://www.cellsignal.com/products/8456.html) from Cell Signaling, antibodies to Flag M2 (http://www.sigmaaldrich.com/catalog/product/sigma/f1804) and c-Myc (http://www.sigmaaldrich.com/catalog/product/sigma/c3956) from Sigma, antibodies to Srebp1c (http://www.novusbio.com/SREBP1-Antibody-2A4_NB600-582.html) from Novus and antibodies to Val1744-cleaved Notch1 (http://www.abcam.com/Notch1-antibody-Cleaved-Val1744-ab52301.html) from Abcam. All antibodies were used at 1:1,000 dilution in Tris-buffered saline plus Tween-20 (TBS-T) containing 1% BSA, except for the antibodies to Flag M2 (1:5,000, TBS-T and 1% BSA) and c-Myc (1:3,000, TBS-T and 1% BSA).

***In vivo* inhibitor studies.** We suspended dibenzazepine (Syncom; 2 μmol per kg body weight), a GSI, and rapamycin (Enzo; 2 mg per kg body weight) in vehicle (0.5% Methocel E4M (wt/vol; Colorcon) and 0.1% Tween-80 (Sigma) solution) and sonicated for 2 min to achieve a homogeneous suspension before daily (for 5 d) intraperitoneal injection[49].

Experimental animals. We crossed albumin-*cre*[20], *Rbpj*$^{flox/flox}$ (ref. 50) and *Foxo1*$^{flox/flox}$ (ref. 51) mice on a C57BL/6 background to generate albumin-*cre*; *Rbpj*$^{flox/flox}$ (*L-Rbpj*), albumin-*cre*; *Foxo1*$^{flox/flox}$ (*L-Foxo1*) and albumin-*cre*; *Rbpj*$^{flox/flox}$; *Foxo1*$^{flox/flox}$ (*L-Rbpj/Foxo1*) mice; the genotyping primers were previously described[20], and only male mice were studied. Mice were weaned to either standard chow (Purina Mills #5053) or HFD (Harlan Laboratories TD.06414). Male wild-type C57BL/6 (strain #662) and male leptin-deficient *ob/ob* (strain #632) mice were purchased from Jackson Labs. The Columbia University Institutional Animal Care and Use Committee approved all animal procedures.

Metabolic analyses. We measured blood glucose concentration by glucose meter (OneTouch) and plasma insulin concentration by ELISA (Millipore). We performed glucose tolerance tests after a 16-h (6 p.m. to 10 a.m.) fast using intraperitoneal injection of 2 g per kg body weight glucose. We extracted hepatic lipids[52], normalized them to either liver weight or protein content and confirmed them visually by Oil Red O staining of snap-frozen liver sections. We used colorimetric assays to measure triglyceride (Thermo), cholesterol E (Wako) and nonesterified fatty acid (Wako) content. We determined hepatic *de novo* lipogenesis by measuring the amount of newly synthesized fatty acid, as resolved by thin-layer chromatography (TLC), in the liver 1 h after intraperitoneal injection of 1 mCi of ^3H_2O (ref. 26). The triglyceride secretion rate was measured after injection of Poloxamer 407 with serial measurement of plasma triglycerides[53].

Hepatocyte studies. We isolated and cultured primary mouse hepatocytes as described[17]. For gene and protein expression studies, we pretreated hepatocytes with 50 nM rapamycin (Cell Signaling) or vehicle for 30 min, followed by treatment for 6 h with 10 nM insulin (Sigma). We measured fatty acid oxidation as described[54] with the following modifications: primary hepatocytes were incubated in serum-free medium with 1.5% fatty acid–free BSA (Sigma) containing 0.1 mM cold oleic acid and 1 μCi ^{14}C-oleic acid (PerkinElmer Life Sciences) for 4 h. Labeled medium was transferred to flasks; 200 μl of 70% perchloric acid was injected into the bottom of the flask, 100 μl of 1 M KOH was injected onto filter paper held by a center well and the flasks were incubated for an additional 1 h. Trapped $^{14}CO_2$ on the alkalinized filter paper was measured as described[54]. We measured lipogenesis as described[44] with the following modifications: hepatocytes were stimulated with 10 nM insulin in serum-free DMEM for 2 h and then labeled with ^{14}C-acetate (PerkinElmer Life Sciences) for 2 h. After incubation with 3:2 hexane:isopropanol for 3 h, extracted lipids were dried under N_2 gas and then resuspended in 2:1 chloroform:methanol before separation of lipid species by TLC and counting of labeled triglycerides. Counts were normalized to the total cellular protein. All primary hepatocyte experiments were finished within 36 h after plating.

Quantitative RT-PCR. We isolated RNA with TRIzol (Invitrogen) or an RNeasy Mini Kit (Qiagen), synthesized cDNA with Superscript III RT (Invitrogen) and performed quantitative PCR with a DNA Engine Opticon 2 System (Bio-Rad) and DyNAmo HS SYBR green (New England Biolabs). mRNA levels were normalized to 18s using the ΔΔC(t) method and are presented as relative transcript levels[21]. Primer sequences are available on request.

Adenovirus studies. The N1-IC, Notch decoy (1-24), Fc and GFP adenoviruses have been described[17,30,55]. We transduced primary hepatocytes or HEK293 cells at a multiplicity of infection (MOI) of 5 and FAO hepatoma cells at an MOI of 200 to achieve 90–100% infection efficiency as assessed by GFP expression. For *in vivo* studies, we injected 1×10^9 purified viral particles (Viraquest) per g body weight through the orbital sinus; we performed metabolic analysis on days 3–5 and euthanized the mice at day 7 or 14 after injection. We limited our analyses to mice showing twofold to fivefold hepatic Notch1 overexpression or detectable hepatic Notch decoy or Fc expression by western blotting.

Luciferase assays. We transfected (Lipofectamine 2000, Invitrogen) FAO hepatoma cells or primary hepatocytes with a luciferase construct (Addgene, 8890) containing the proximal (−220 to +25) *Fasn* promoter sequence[56]. In some experiments we cotransfected plasmids containing shRNA to Raptor (Addgene, 21339 or 21340) or Rictor (Addgene, 21341) with scrambled shRNA (Addgene, 1864) as a control[32] and/or transduced cells with N1-IC or control (Fc) adenovirus. Twenty-four hours after transfection, FAO cells or primary hepatocytes were transferred to serum-free medium for 16 h and then treated with 10 nM insulin (Sigma) for 6 h before lysis and luciferase measurements as described[56].

Immunoprecipitation. We lysed HEK293 cells, FAO cells and primary hepatocytes in 0.3% or 0.6% CHAPS-containing buffer[34], followed by immunoprecipitation for 2 h at 4 °C and overnight elution before western blot analysis[57].

Statistical analyses. We used two-way ANOVA to analyze the data. All western blots were quantified using NIH ImageJ software. All data are shown as the means ± s.e.m.

49. van Es, J.H. *et al.* Notch/γ-secretase inhibition turns proliferative cells in intestinal crypts and adenomas into goblet cells. *Nature* **435**, 959–963 (2005).
50. Fujikura, J. *et al.* Notch/Rbp-j signaling prevents premature endocrine and ductal cell differentiation in the pancreas. *Cell Metab.* **3**, 59–65 (2006).
51. Paik, J.H. *et al.* FoxOs are lineage-restricted redundant tumor suppressors and regulate endothelial cell homeostasis. *Cell* **128**, 309–323 (2007).
52. Folch, J., Lees, M. & Sloane Stanley, G.H. A simple method for the isolation and purification of total lipides from animal tissues. *J. Biol. Chem.* **226**, 497–509 (1957).
53. Millar, J.S., Cromley, D.A., McCoy, M.G., Rader, D.J. & Billheimer, J.T. Determining hepatic triglyceride production in mice: comparison of poloxamer 407 with Triton WR-1339. *J. Lipid Res.* **46**, 2023–2028 (2005).
54. Li, G., Hernandez-Ono, A., Crooke, R.M., Graham, M.J. & Ginsberg, H.N. Effects of antisense-mediated inhibition of 11β-hydroxysteroid dehydrogenase type 1 on hepatic lipid metabolism. *J. Lipid Res.* **52**, 971–981 (2011).
55. Nakae, J. *et al.* The forkhead transcription factor Foxo1 regulates adipocyte differentiation. *Dev. Cell* **4**, 119–129 (2003).
56. Kim, J.B. *et al.* Nutritional and insulin regulation of fatty acid synthetase and leptin gene expression through ADD1/SREBP1. *J. Clin. Invest.* **101**, 1–9 (1998).
57. Qiang, L. *et al.* Brown remodeling of white adipose tissue by SirT1-dependent deacetylation of Pparγ. *Cell* **150**, 620–632 (2012).

doi:10.1038/nm.3259